

# Cobalt nanoparticles as reusable catalysts for reduction of 4-nitrophenol under mild conditions

ARIJIT MONDAL<sup>1</sup>, ASISH MONDAL<sup>1</sup>, BIBHUTOSH ADHIKARY<sup>2</sup>  
and DEB KUMAR MUKHERJEE<sup>1,\*</sup>

<sup>1</sup>Department of Chemistry, Ramsaday College, Howrah 711401, India

<sup>2</sup>Department of Chemistry, Indian Institute of Engineering Science and Technology, Shibpur, Howrah 711103, India

MS received 26 November 2015; accepted 27 June 2016

**Abstract.** Facile reduction of *p*-nitrophenol to *p*-aminophenol by sodium borohydride catalysed by cobalt nanoparticles (CoNPs) has been discussed. A simple approach has been made to synthesize highly active and ordered structures of CoNPs. The air-stable nanoparticles were prepared from cobalt sulphate using tetrabutyl ammonium bromide as surfactant and sodium borohydride as reductant. The cobalt nanocolloids in aqueous medium were found to be efficient reusable catalysts for the *p*-nitrophenol reduction. Palladium nanoparticles prepared from palladium chloride and the same surfactant were found to reduce *p*-nitrophenol but lose their catalytic efficiency after recovery. Based on chemical and kinetic studies, an attempt has been made to elucidate the mechanism of *p*-nitrophenol reduction using these nanoclusters.

**Keywords.** Cobalt nanoparticles; 4-nitrophenol; reduction; aggregation; recyclability.

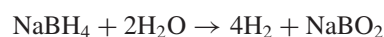
## 1. Introduction

Metal nanoparticles have received tremendous interest in the scientific literature because of their unique chemical and physical characteristics that are different from their bulk counterparts [1]. Several methods have been developed for synthesis of transition metal nanoparticles [2]. In recent years several approaches such as pyrolysis [3,4], solvothermal [5], hydrothermal decomposition [6], modified polyol processes [7] and template-based methods [8] have been developed to synthesize cobalt crystals with different morphologies. Some efforts have been focused on exploring the relations between their shapes and properties. There is however no report of a very simple and quick method to prepare cobalt nanoparticles (CoNPs) that are reusable catalysts for reduction of organic functional moieties under mild conditions [9,10].

Catalysis has revolutionized the field of manufacturing of chemicals. One such manufacturing process is reduction of organic molecules by catalytic hydrogenation. Nitrophenols are considered to be amongst the most prevalent organic pollutants in waste water generated from agricultural and industrial sources [11–13]. The US Environmental Protection Agency has reported nitrophenols as one of the most hazardous and toxic pollutants [14]. Therefore, the development of an effective and ecofriendly method to remove them from water is of great importance. In the synthesis of various analgesic and antipyretic drugs such as paracetamol, acetanilide and phenacetin, 4-aminophenol (4-AP), the reduced product

from 4-nitrophenol (4-NP), is an important intermediate [15]. It is also the main ingredient in the synthesis of industrial dyes, marketed as a photographic developer, and its oxalate salt has been reported to be a corrosion inhibitor [11].

It has been noted that *p*-aminophenol could be obtained by methods such as hydrogenation of nitrobenzene involving molecular rearrangement of phenylhydroxylamine intermediate in the presence of iron–acid [16], catalytic amination of hydroquinone [17], electrochemical reduction of nitrophenols [18], etc. Methods for the catalytic hydrogenation of 4-NP in solvents such as ethanol at relatively high temperature and high hydrogen pressure have been reported [19,20]. The disadvantages of such methods include formation of aniline as a side product, long reaction time and extensive methodology involved during usage of hydrogenation of 4-NP [21,22]. Such methods are also associated with serious pollution problem due to the formation of large amounts of metal oxide sludge and corrosion of the reaction vessels. In recent times, based on the requirements such as greener route and safer operation, direct environmentally friendly catalytic conversion routes have been developed for the conversion of *p*-nitrophenol to *p*-aminophenol in aqueous medium under mild conditions. One such route by which *p*-aminophenol is obtained involves direct hydrogenation of 4-NP using sodium borohydride, which is a mild agent, and the reaction can be conducted in an aqueous medium [23]. This method is relatively simple and clean compared with the above-mentioned methods. But the sluggish self-hydrolysis of NaBH<sub>4</sub> affects the rate of hydrogenation of the nitro-compound [24]:



\* Author for correspondence (debkumarmukherjee@rediffmail.com)

Many reports are available on the application of metal nanoparticles as catalysts for the hydrogenation of 4-NP in the presence of  $\text{NaBH}_4$  [23,25–27]. Metal-oxide-supported metal nanoparticles have been tested as catalysts for the conversion of *p*-nitrophenol to *p*-aminophenol. Pd nanoparticles dispersed in alumina have been reported [28] with  $\text{NaBH}_4$  as the reducing agent. Yu *et al* [29] used PVP-stabilized Pt nanoparticles and  $\text{CeO}_2$ -supported Pt nanoparticles as catalysts. In such catalyst-mediated reactions even though PVP-stabilized Pt nanoparticles showed higher activity than the Pt/ $\text{CeO}_2$  hybrid, it lost its catalytic activity during the course of recyclability. Although nanomaterials have their own advantages, the protocol is not commercially viable due to multi-step nanoparticle preparation method and the tedious process of catalyst regeneration from the solvent system [23,25–27].

## 2. Experimental

### 2.1 Chemicals and materials

All chemicals were of reagent grade and used without further purification. Cobalt sulphate ( $\text{CoSO}_4$ ), tetrabutyl ammonium bromide (TBAB), sodium borohydride ( $\text{NaBH}_4$ ), 4-NP and acetone were purchased from Merck-India.

### 2.2 Preparation of TBAB-stabilized CoNPs from $\text{CoSO}_4$

To a screw-capped vial with a stirring bar were added 32 mg of cobalt sulphate ( $113.83 \mu\text{mol}$ ), 38 mg tetrabutyl ammonium bromide ( $117.87 \mu\text{mol}$ ) and 4 ml of deionized water. After adding deionized aqueous solution of  $\text{NaBH}_4$  (0.1 M) dropwise, the mixture was stirred at room temperature for 1 h, and then the aqueous solution was decanted off. Subsequently, the black coloured TBAB-stabilized CoNPs were washed with water ( $5 \times 5.0 \text{ ml}$ ) and acetone ( $5 \times 5.0 \text{ ml}$ ) 4–5 times. The shiny black particles were dried at room temperature in a desiccator for 24 h before use as catalysts (figure 1).



$\text{CoSO}_4$  solution before reaction with  $\text{NaBH}_4$



After addition of  $\text{NaBH}_4$

**Figure 1.** Preparation of magnetic cobalt nanoparticles from  $\text{CoSO}_4$ .

### 2.3 Characterization

High-resolution transmission electron microscopy (HRTEM) images of CoNPs were obtained and are shown in figure 2 (HRTEM, CM 30 microscope operating at 200 kV and expanded to  $470 \text{ pixels cm}^{-1}$ ). TEM samples were prepared by dispersing CoNPs in acetone for 45 min in a sonicator; then the solution was withdrawn using a hypothermal syringe; one drop of the solution was poured on a carbon-coated copper grid and left to dry. The ultraviolet–visible (UV–vis) absorption spectra were measured at room temperature on an INTECH spectrophotometer using solutions in a 1 cm quartz absorption cell over wavelength 350–700 nm range.

### 2.4 Catalytic degradation process

In a representative degradation experiment, the TBAB-stabilized CoNPs (3 mg) and an aqueous solution of  $\text{NaBH}_4$

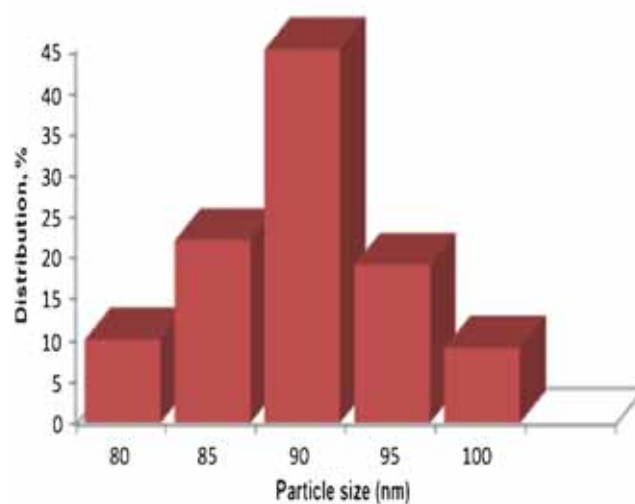
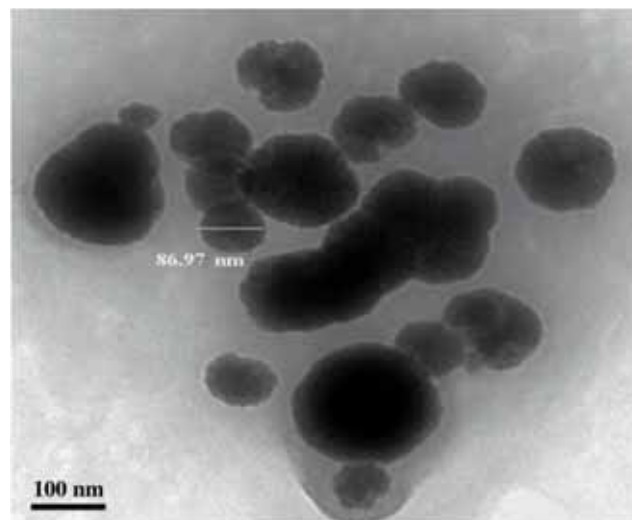


**Figure 2.** TEM image of synthesized cobalt nanoclusters.

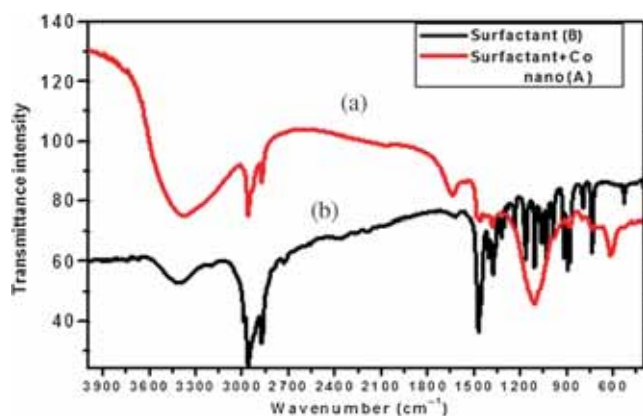
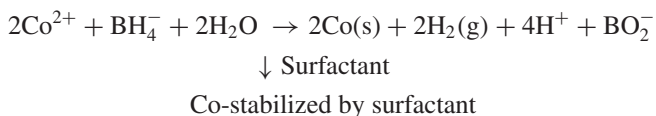


**Figure 3.** FTIR spectra: (a) TBAB-capped CoNPs and (b) TBAB surfactant.

(10 ml,  $2 \times 10^{-5}$  M) were rapidly introduced into an aqueous solution of *p*-nitrophenol (10 ml,  $1 \times 10^{-6}$  M) and then the whole mixture was allowed to react for 2 min at room temperature under atmospheric pressure. Thereafter the whole mixture was subjected to UV–vis spectral analysis at room temperature in the visible range. The concentration of *p*-nitrophenol was quantified by measuring the absorption intensity at  $\lambda_{\max} = 390$  nm. When required, sample solutions were diluted five times before optical density measurement was made.

### 3. Results and discussion

The formation of CoNPs during the reaction process was noticeable by dramatic colour change of the cobalt sulphate solution after the introduction of the reducing agent. The overall reaction proposed for this process is as follows:



The presence of the surfactant on the surface of CoNPs can be explained by comparing the FTIR data (figure 3).

The surface binding interaction study of TBAB-capped CoNPs was carried out by recording FTIR spectra in the range of  $4000\text{--}500\text{ cm}^{-1}$ , which are shown in figure 3. The characteristic bands of pure TBAB can be divided into two regions, two absorption bands in the range of  $2958\text{--}2874\text{ cm}^{-1}$ , which are attributed to symmetric and anti-symmetric stretching of the aliphatic group ( $\text{CH}_2$ , tail), and another band at  $1622\text{ cm}^{-1}$ , assigned to nitrogen group (head group) of the TBAB molecules. TEM images suggest that these as-prepared CoNPs are of large sizes compared with those reported earlier for palladium and platinum by our group. The size distribution studied for 64 such particles suggests that the average size lies in the range  $90\text{--}95$  nm for cobalt nanocolloids and they do not coagulate into the precipitated form when left in acetone solution for almost 24 h.

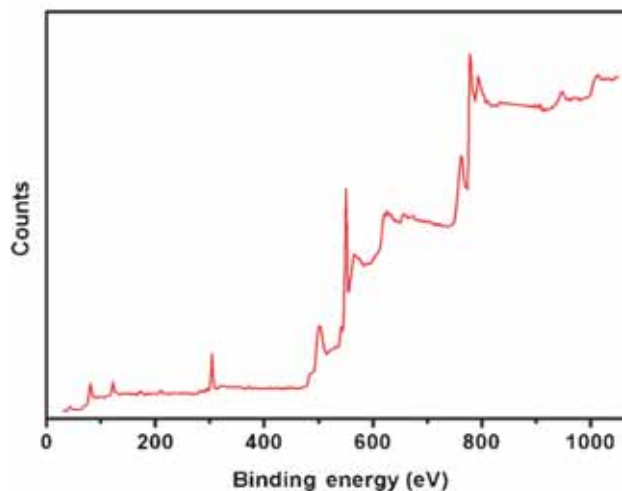
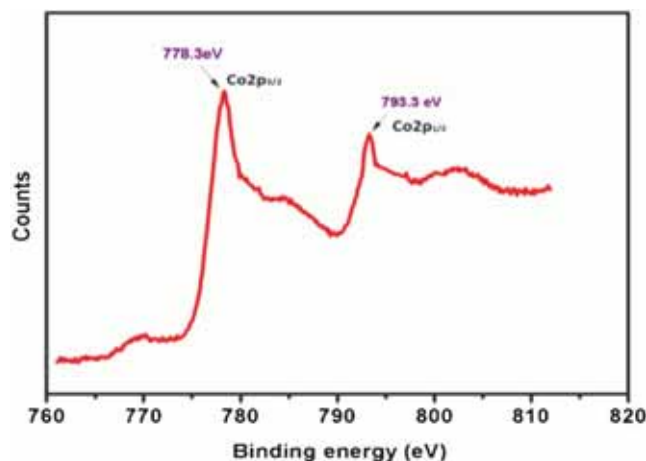


**Figure 4.** XPS of synthesized cobalt nanoparticles.

#### 3.1 X-ray photoelectron spectroscopy of CoNPs

X-ray photoelectron spectroscopy (XPS) was used to examine the oxidation state of the synthesized CoNPs. The  $\text{Co}2p_{1/2}$  and  $\text{Co}2p_{3/2}$  peaks of TBAB-stabilized CoNPs were measured on an Escalab 5 spectrometer with monochromated Mg X-rays at 10 kV. Samples for XPS were prepared by spreading several drops of cobalt dispersion in acetone on standard Si (111) wafers with a 150-nm-thick  $\text{SiO}_2$  layer and allowing the solvent to slowly evaporate. A vacuum-transfer vessel was used to carry the sample from the drying box to the chamber without exposing the sample to air any more. The surface of the as-prepared nanoparticle was then investigated and the results are given in figure 4. Various oxidation peaks of cobalt that have been reported in the literature [30] are as follows: 778.3 and 793.3 eV for  $\text{Co}^0$ , 780.4 and 795.8 eV for  $\text{Co}^{2+}$  and 778.5 and 794.2 eV for  $\text{Co}^{3+}$ . In the present case, the nanoparticle exhibits  $\text{Co}2p_{3/2}$  core level peak at a binding energy of 778.3 eV, and  $\text{Co}2p_{1/2}$  at 793.3 eV with a difference of 15 eV, which can be attributed to the presence of typical valence state of  $\text{Co}^0$  (figure 4).

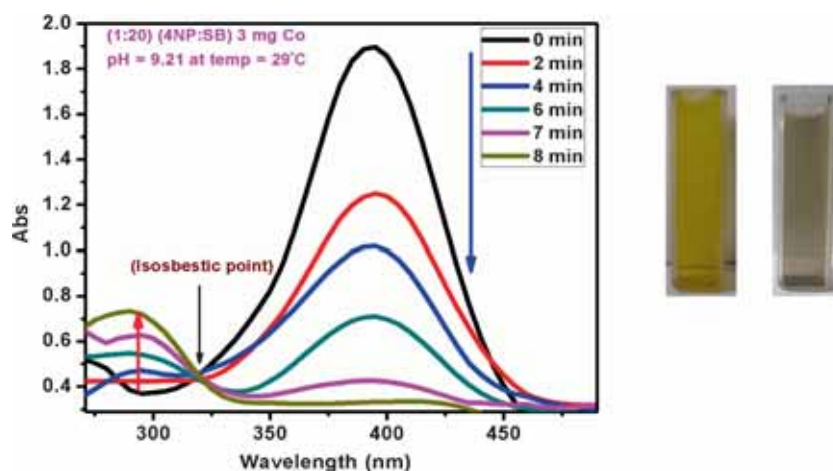


Figure 5. Reduction of 4-nitrophenol by CoNPs under mild conditions.

### 3.2 Catalytic activity of CoNPs during reduction of 4-NP



To investigate the catalytic activity of CoNPs, the cobalt nanosized particles were first employed in the degradation of 4-NP in the presence of sodium borohydride. The progress of the catalytic degradation of 4-NP can be easily monitored by the decrease in optical density at the wavelength of the absorbance of 4-NP (figure 5). It can be seen that the absorption band of 4-NP at 390 nm decreases gradually with the reaction time and yellow colour of the mixture vanished in 8 min when the spherical CoNPs were used. In the control experiment without any catalyst, an intense absorption peak at 390 nm was still observed even after 1 day. Cobalt sulphate used as a catalyst in place of nanoparticles has no effect and the spectrum is almost similar to that obtained during degradation of 4-NP in the presence of sodium borohydride only. It is therefore true that the presence of both borohydride and nanoparticles is required for effective reduction of the substrate.

### 3.3 Effect of molar ratio of 4-NP and NaBH<sub>4</sub> on catalytic reduction

The effect of NaBH<sub>4</sub> concentration on the catalytic reduction was also studied. Here, concentration of 4-NP and amount of catalyst were kept constant and the NaBH<sub>4</sub> concentration was varied (figure 6). Thereafter we have optimized the

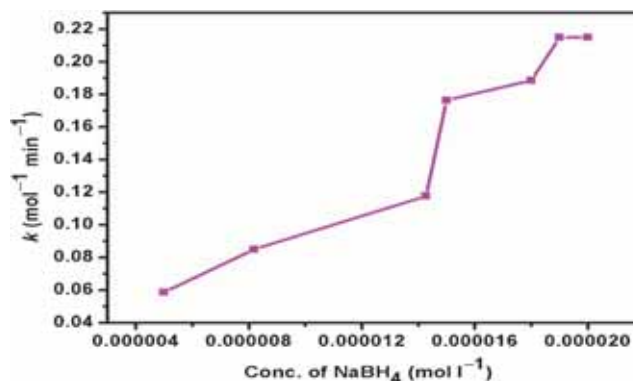


Figure 6. Reduction of 4-NP with varied concentration of NaBH<sub>4</sub> at 29°C and pH = 9.21.

concentration of NaBH<sub>4</sub> ( $2 \times 10^{-5}$  M) for the present study. It was observed that in the concentration range ( $5 \times 10^{-6}$  to  $2 \times 10^{-5}$  M) of NaBH<sub>4</sub>, the rate increases with the increase in BH<sub>4</sub><sup>-</sup> concentration, while ( $2 \times 10^{-5}$  M) onwards of NaBH<sub>4</sub> concentration the rate remains almost constant. Kinetics of the reduction of 4-NP has been shown to be of first order with respect to substrate concentration [31–33].

### 3.4 Effect of CoNPs dosage

The effect of the CoNPs on reduction rate of 4-NP has been presented in figure 7. It was found that when the CoNPs dosage increased, the concentration of *p*-nitrophenol decreased rapidly and the degradation to 90% is over in just 8 min when 3 mg ( $2 \times 10^{-5}$  metal content l<sup>-1</sup>) is used. This is expected because, with more CoNPs used, there will be more active surface sites available for reaction with *p*-nitrophenol. The increased CoNPs though increases the reduction rate drastically, it becomes difficult to follow the kinetic studies by monitoring absorbance change.

### 3.5 Effect of pH on catalytic reduction

In the representative experiment the degradation of 4-NP was carried out at 29°C and pH = 9.21. The effect of high and low pH on degradation rate was studied keeping the amount of CoNPs fixed and other parameters unchanged. The pH of the aqueous solution was maintained by adding requisite amounts of HCl (0.1 N) and aqueous NaOH solution (0.1 N). It is quite evident that the degradation of 4-NP is fast enough at pH less than 9 and difficult to be monitored at different time intervals (figure 8). The sodium borohydride aqueous solution is however stable in the alkaline medium and the

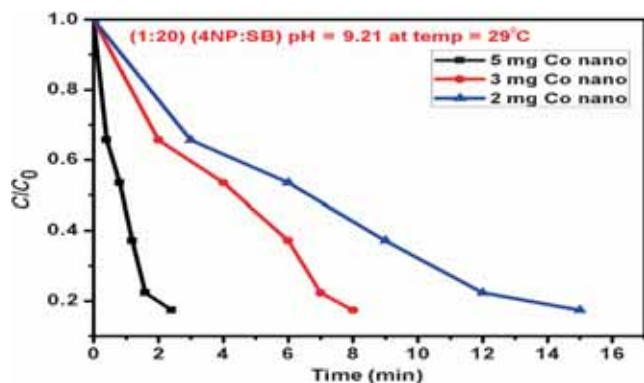


**Figure 7.** Effect of different amounts of nanoparticles during degradation of 4-NP.

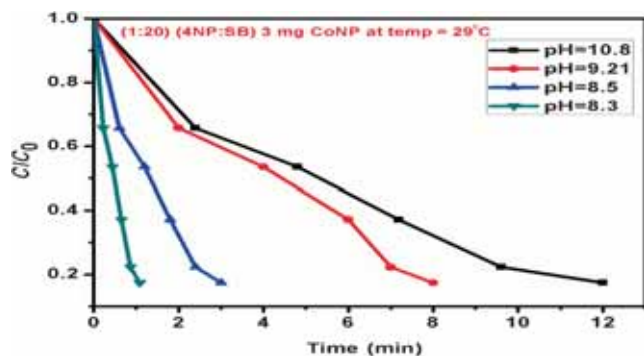


**Figure 8.** Effect of pH on 4-NP degradation using CoNPs.

chances of deprotonation of –OH moiety of 4-NP is reduced at pH > 10.

The enhanced reduction rate of azo dyes with an increase in H<sup>+</sup> concentration (i.e., at low pH) has also been reported by Shih *et al* [34], Soomro *et al* [35] and Mondal *et al* [36].

### 3.6 Effect of temperature

The effect of temperature on the reaction kinetics of 4-NP with CoNPs was investigated over the temperature range 10–50°C as shown in figure 9. The rate constant of *p*-nitrophenol with CoNPs at 48, 38, 29 and 10°C was estimated to be 0.254, 0.222, 0.21 and 0.07 min<sup>-1</sup>, respectively. It is obvious that higher the temperature, faster the collision of these nano-sized particles with the substrate in aqueous solution and hence the reaction occurs at a much faster rate.

A plot of ln *k* vs. 1/*T* using linear least-square analysis has been shown in figure 10. The estimated activation energy for the degradation of *p*-nitrophenol by CoNPs is approximately 61.32 kJ mol<sup>-1</sup>. The value corresponds to that observed during reduction of 4-NP by Lu *et al* [37] using Ag-nano-composite.

### 3.7 Separation of CoNPs and recyclability study

The catalyst can be easily separated from the reaction medium. As CoNPs themselves have magnetic property they get stuck into the magnetic bar used in the system. Aqueous solution was decanted from the reaction vessel and CoNPs on the magnetic bar were dispersed in deionized water using a sonicator. The solution was centrifuged, when all nanoparticles settled at the bottom of the centrifuge tube and the aqueous solution was carefully decanted out. The process was repeated two times, when finely dispersed black particles were obtained.

Recycling experiments were performed to test the reuse of the spherical CoNPs. Catalytic experiments under similar conditions suggest that the regenerated particles possess relatively good activity even in the 5th cycle. The time of degradation of 4-NP with every cycle however increases and almost gets doubled during the 3rd recycle experiment (figure 11). After three consecutive cycles the CoNPs were collected for HRTEM image to study their

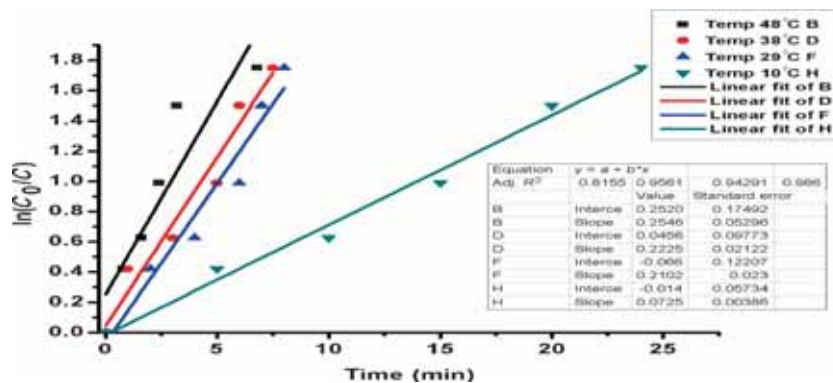


**Figure 9.** Kinetic studies for catalytic reduction of 4-NP by cobalt nanoclusters.

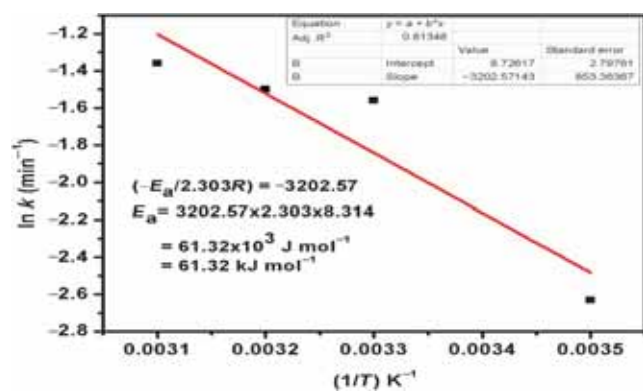


**Figure 10.** Estimation of activation energy for CoNP-catalysed 4-NP degradation.

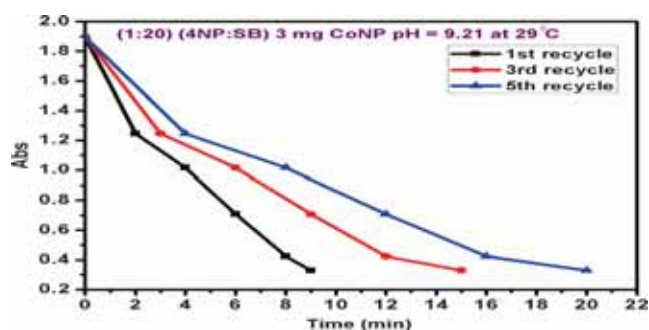


**Figure 11.** Recyclability experiment of cobalt nanoclusters.

particle size distribution and verify whether agglomeration or further degradation of particles has occurred. HRTEM image (figure 12) of the recycled particles showed that no such phenomena have occurred. XRD patterns of fresh cobalt particles and those collected after three catalytic cycles were also identical, which emphasizes the very stable nature of CoNPs.

### 3.8 Comparative study with palladium nanoparticles

Palladium nanoparticles were prepared and characterized by the method followed earlier by our group [38]. These as-prepared particles were then studied for 4-NP reduction under identical conditions.

TEM image and particle size distribution of these nanoclusters prepared from PdCl<sub>2</sub> have been presented in figure 13.

UV-vis spectra for the degradation of 4-NP using palladium nanoclusters as catalyst show that the absorption intensity of the system utilizing Pd nanoparticles decreases rapidly and the reaction gets completed within 12 min (figure 14). The reaction was incomplete when no palladium nanoparticles were used or when palladium chloride was added in place of nanoparticles. The reduction of 4-NP with CoNPs is therefore much faster compared with palladium nanoparticles when the same metal content per litre aqueous solution was used. To recover the palladium nanoparticles for the recycling process, the aqueous solution was first decanted

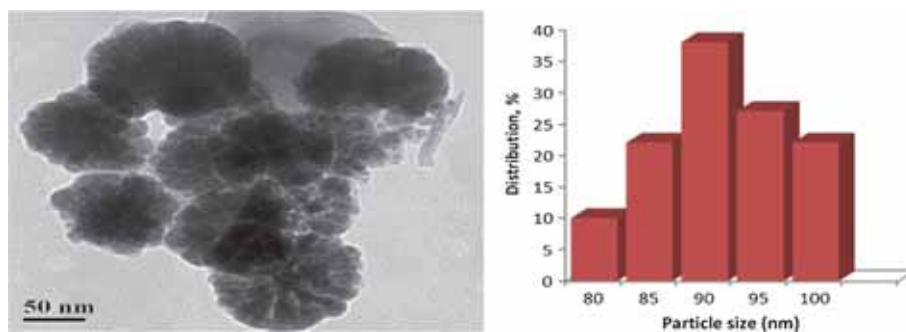


**Figure 12.** Recovered nanoparticles after 3rd catalytic run.

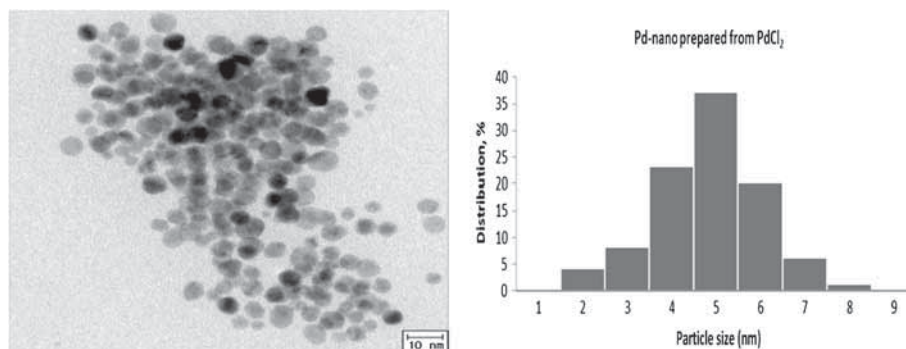


**Figure 13.** TEM image and size distribution of palladium nanoparticles.

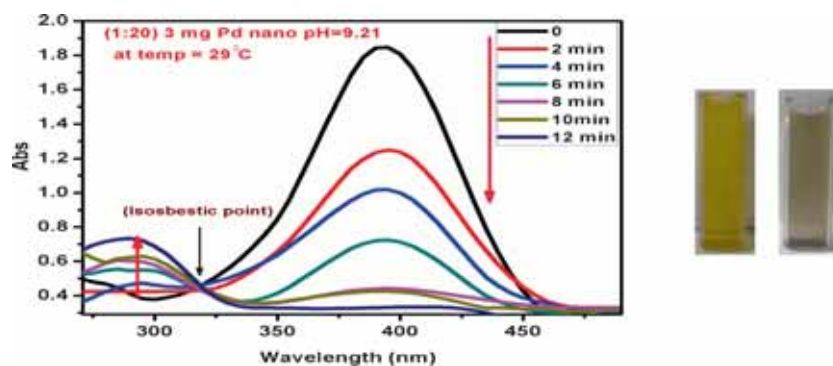


Figure 14. Reduction of 4-nitrophenol by PdNPs under mild conditions.

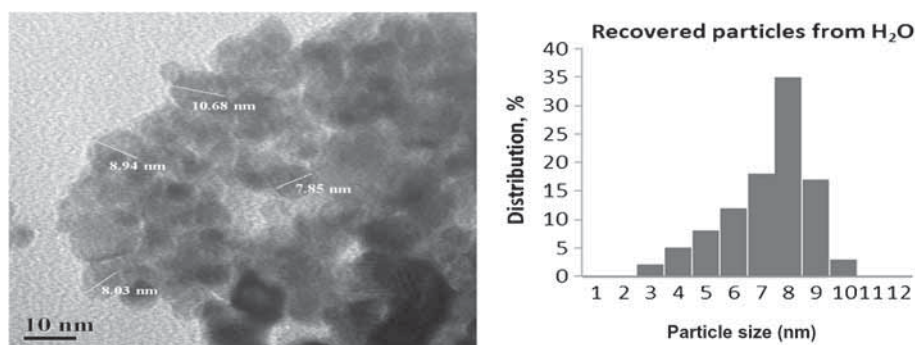
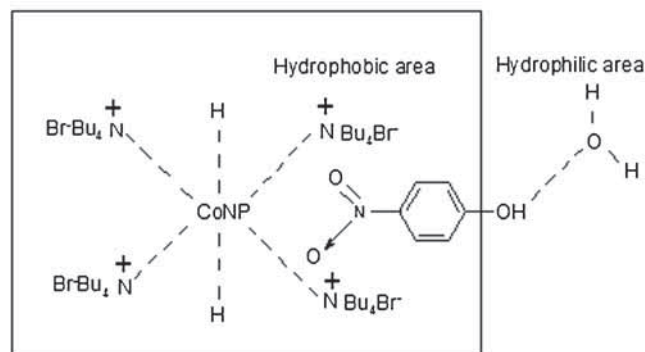
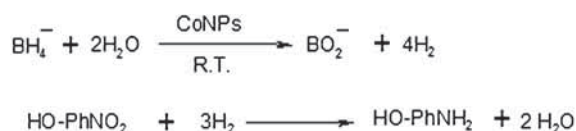


Figure 15. Recovered TEM picture of palladium nanoparticles.

off and similar steps were followed as employed in case of CoNPs. To our surprise we noticed that after 2nd recycling experiment, the degradation time of 4-NP increased considerably. HRTEM of the nanoparticles collected after 1st degradation shows differences as far as average particle size distribution is concerned. Micrographs reveal considerable aggregation of the palladium particles on use and this is reflected in the increase in average size of recovered particles. Palladium particles freshly prepared from  $\text{PdCl}_2$  had on an average a diameter of 4–5 nm and this increased to around  $8 \pm 1$  nm at the end of the first cycle (figure 15). Hence from an industrial point of view we cannot say that palladium nanoclusters are good catalysts. On the other hand, cobalt is a much cheaper material and retains catalytic activity even on prolonged use.

### 3.9 Proposed mechanism of reduction by nanoparticles

In addition to *p*-nitrophenol, *p*-nitrobenzoic acid was also subjected to reduction under similar conditions. It was noticed that *p*-aminobenzoic acid was formed and no other intermediates could be detected by gas chromatography even after 24-h reaction. The nitro-group is chemoselectively reduced, while the carboxylic acid moiety remains unchanged under reduction conditions. The appearance of isosbestic point during reduction of 4-NP (figure 5) suggests that the reaction is indeed clean with no formation of stable intermediates. We therefore proposed that the  $\text{NO}_2^-$



Scheme 1. Proposed pathway for hydrogenation of  $\text{NO}_2^-$  group by nanoparticles protected by surfactant.

group, which lies close to the metal centre in the hydrophobic zone, is reduced but the functional groups extended into the hydrophilic region remain in the unreduced form (scheme 1).

CoNPs having larger particle size could accommodate the coordinated borohydride, substrate and the solvent molecule at its surface sites effectively and reduction occurs at the

surface of these nanoparticles as proposed by earlier workers in their published studies [39–42]. The reaction is facilitated by increased borohydride concentration (reference figure 6) and at an alkaline pH, where the aqueous solution containing the borohydride species remains stable. BET measurement of surface areas and TEM studies clearly suggest that the regenerated cobalt nanoclusters do not lose their surface characteristics or size during the work-up procedures and therefore function as recyclable catalysts. Under similar situations the surface sites change in case of palladium nanoclusters due to agglomeration phenomenon and they lose their effectiveness on recycling.

#### 4. Conclusion

We have shown here that the spherical cobalt nanoparticles can catalyse the degradation of 4-NP in the presence of sodium borohydride, producing a remarkable enhancement in the reaction rate. It is highly air stable and represents an inexpensive, eco-friendly alternative noble metal catalyst suitable for waste water treatment. Further reactions involving reduction of organic functionalities employing metal nanoclusters will be undertaken in future.

#### Acknowledgement

We are grateful to the Department of Chemistry, R.S. College, and Indian Institute of Engineering Science and Technology for all instrumental support and to the University Grants Commission-New Delhi for providing financial support and scholarship to A.M.

#### References

- [1] Daniels M and Astruc D 2004 *Chem. Rev.* **104** 293
- [2] Cushing B L, Kolesnichenko V L and O'Connor C J 2004 *Chem. Rev.* **104** 3893
- [3] Guo L, Liang F, Wen X G, Yang S H, He L, Zheng W Z, Chen C P and Zhong Q P 2007 *Adv. Funct. Mater.* **17** 425
- [4] Liu S H, Gao H T, Ye E Y, Low M, Lim S, Zhang S Y, Lieu X H, Tripathy S, Tremel W and Han M Y 2010 *Chem. Commun.* **46** 4749
- [5] Wang X, Yuan F L, Hu P, Hu L J and Bai L Y 2008 *J. Phys. Chem. C* **112** 8773
- [6] Cao F, Deng R P, Tang J K, Song S Y, Lei Y Q and Zhang H J 2011 *CrystEngComm* **13** 223
- [7] Dakhloui A, Smiri L S, Babadjiam G, Schoenstein F, Molinié P and Jouini N 2008 *J. Phys. Chem. C* **112** 14348
- [8] Xia L X, Zhao H, Liu G, Hu X, Liu Y, Li J, Yang D and Wang X 2011 *Colloids Surf. A: Physicochem. Eng. Aspects* **384** 358
- [9] Y B CaO, Zhang X, Fan J M, Hu P, Bai L Y, Zhang H B, Yuan F L and Chen Y F 2011 *Cryst. Growth Des.* **11** 472
- [10] Zhang P, An Q, Guo J and Wang C C 2013 *J. Colloid Interface Sci.* **389** 10
- [11] Kkroschwitz J I (ed) 1995 *Kirk-Othmer encyclopedia of chemical technology vol 2, 4th edn* (USA: Wiley Interscience) p 580
- [12] Mori T, Watanuki T and Kashiwaguru T 2007 *Environ. Toxicol.* **22** 58
- [13] Li C M, Taneda S, Suzuki A K, Furuta C, Watanabe G and Taya K 2006 *Appl. Pharmacol.* **217** 1
- [14] Feng Z V, Lyon J L, Croley J S, Crooks R M, Bout D A V and Stevenson K J 2009 *J. Chem. Educ.* **86** 368
- [15] Rode C V, Vaidya M J, Jaganathan R and Chaudhari R V 2001 *Chem. Eng. Sci.* **56** 1299
- [16] Polat K, Aksu M L and Pekel A T 2002 *J. Appl. Electrochem.* **32** 217
- [17] Bean F and Thomas S 1945 *US Patent 2* **376** 112
- [18] Abbar A H, Sulaymon A H and Jalhoom M G 2007 *Electrochim. Acta* **53** 1671
- [19] Du Y, Chen H, Chen R and Xu N 2004 *Appl. Catal. A* **277** 259
- [20] Vaidya M J, Kulkarni S M and Chaudhari R V 2003 *Org. Process Res. Dev.* **7** 202
- [21] Farhadi S and Siadatnasab F 2011 *J. Mol. Catal. A: Chem.* **339** 108
- [22] Holtzclaw C and Bryan W 1965 *US Patent 3* **177** 256
- [23] Liu P and Zhao M 2009 *Appl. Surf. Sci.* **255** 3989
- [24] Kojima Y, Suzuki K, Fukumoto K, Sasaki M, Yamamoto T, Kawai Y and Hayashi H 2002 *Int. J. Hydrogen Energy* **27** 1029
- [25] Chang Y C and Chen D H 2009 *J. Hazard. Mater.* **165** 664
- [26] Wu Y, Zhang T, Zheng Z, Ding X and Peng Y 2010 *Mater. Res. Bull.* **45** 513
- [27] Kuroda K, Ishida T and Haruta M 2009 *J. Mol. Catal. A: Chem.* **298** 7
- [28] Arora S, Kapoor P and Singla M L 2010 *React. Kinet. Mech. Catal.* **99** 157
- [29] Yu T, Zeng J, Lim B and Xia Y 2010 *Adv. Mater.* **22** 5188
- [30] Rong M Z, Zhang M Q, Wang H B and Zeng H M 2002 *Appl. Surf. Sci.* **200** 76
- [31] Chen X, Zheng Z, Ke X, Jaatinen E, Xie T, Wang D, Guo C, Zhao J and Zhu H 2010 *Green Chem.* **12** 414
- [32] Deshmukh S P, Dhokale R K, Yadav H M, Achary S N and Delekar S D 2013 *Appl. Surf. Sci.* **273** 676
- [33] Yang G C and Lee H L 2005 *Water Res.* **39** 884
- [34] Shih Y H, Tso C P and Tung L Y 2010 *J. Environ. Eng. Manag.* **20** 137
- [35] Soomro R A, Sherazi S T H, Sirajuddin N, Raza M, Shah N H K, Hallam K R and Shah A 2014 *Adv. Mater. Lett.* **5** 191
- [36] Mondal A, Adhikary B and Mukherjee D K 2015 *Colloids Surf. A: Physicochem. Eng. Aspects* **482** 248
- [37] Lu Y, Mei Y, Walker R, Ballauff M and Drechsler M 2006 *Polymer* **47** 4985
- [38] Mondal A, Das A, Adhikary B and Mukherjee D K 2014 *J. Nano Part. Res.* **16** 1
- [39] Gu S, Wunder S, Lu Y, Ballauff M, Fenger R, Rademan K, Jaquet B and Zacccone A 2014 *J. Phys. Chem. C* **118** 18618
- [40] Wunder S, Polzer F, Lu Y, Mei Y and Ballauff M 2010 *J. Phys. Chem. C* **114** 8814
- [41] Wunder S, Lu Y, Albrecht M and Ballauff M 2011 *ACS Catal.* **1** 908
- [42] Antonels N C and Meijboom R 2013 *Langmuir* **29** 13433